Impedimetric melanoma invasion assay device using a simple paper membrane and stencil-printed electrode on PMMA substrate

Pupinyo, Naricha; Heiskanen, Arto; Chailapakul, Orawon; Gorton, Lo; Emnéus, Jenny; Laiwattanapaisal, Wanida

Published in:
Sensing and Bio-Sensing Research

Link to article, DOI:
10.1016/j.sbsr.2020.100354

Publication date:
2020

Document Version
Publisher's PDF, also known as Version of record

Sensing and Bio-Sensing Research 29 (2020) 100354

Contents lists available at ScienceDirect

Sensing and Bio-Sensing Research

journal homepage: www.elsevier.com/locate/sbsr

Impedimetric melanoma invasion assay device using a simple paper membrane and stencil-printed electrode on PMMA substrate

Naricha Pupinyo[a], Arto Heiskanen[b], Orawon Chailapakul[c], Lo Gorton[d], Jenny Emnéus[b,*], Wanida Laiwattanapaisal[c,e,**]

[a] Graduate Program in Clinical Biochemistry and Molecular Medicine, Department of Clinical Chemistry, Faculty of Allied Health Sciences, Chulalongkorn University, Bangkok 10330, Thailand
[b] Department of Biotechnology and Biomedicine, Technical University of Denmark, Produktionstorvet, Building 423, room 122, 2800 Kgs. Lyngby, Denmark
[c] Electrochemistry and Optical Spectroscopy Center of Excellence (EOSCE), Department of Chemistry, Faculty of Science, Chulalongkorn University, Bangkok, Thailand
[d] Department of Biochemistry and Structural Biology, Lund University, P.O. Box 124, SE-221 00 Lund, Sweden
[e] Biosensors and Bioanalytical Technology for Cells and Innovative Testing Device Research Unit, Department of Clinical Chemistry, Faculty of Allied Health Sciences, Chulalongkorn University, Bangkok, Thailand

ARTICLE INFO

Keywords:
3D cell culture
Paper-based cell culture
Stencil-printed electrode
Impedance monitoring
Invasion assay
Melanoma

ABSTRACT

The transwell assay is currently the most popular approach to studying cellular invasion due to its ease of use and readout, and the possibility for quantitative measurements. However, it only allows end-point measurements without the possibility for real-time tracking of the dynamics of cell movement during an invasion. Moreover, it requires cell labeling, and construction of customized devices is hampered by the commercial standard membrane inserts, only available in certain designs. Recently, paper has been used as a scaffold for three-dimensional (3D) cell cultures. Because of its microfibrous structure and easy handling, it could be a versatile alternative as a membrane insert in customized devices. Here, we develop a low-cost real-time invasion assay device using paper as an alternative membrane insert. The device was designed for two-electrode impedance measurements and fabricated using CNC micromilling. It also comprised a disposable low-cost stencil-printed working electrode on a poly(methyl methacrylate) substrate below the membrane and glassy carbon counter electrode above the membrane inserted in a specially designed lid. Thus, the impedance measurements during cell invasion addressed the entire membrane. We demonstrated the function of the device by monitoring the invasion of B16 melanoma 4A5 cells from a mouse using insulin growth factor-1 as the chemoattractant. The cell invasion on paper was visualized using scanning electron microscopy and confocal microscopy with *Z*-stack 3D imaging. Melanoma cell invasion could be observed within 7 h after the chemoattractant treatment, which was faster than the conventional assay and less likely to be influenced by cell proliferation.

1. Introduction

Understanding the cancer metastatic mechanism is crucial for the development of targeted therapies [1]. To study the cancer invasion mechanism responding to different chemokines, the transwell assay is the most common method used nowadays due to its scalability and simple end-point readout [2]. However, the transwell assay is still based on the 2D formation of cells, which fails to recapitulate the natural behavior of cells *in vivo* [3]. Besides, the experimental setup relies on the use of a commercial membrane insert, which was available in certain sizes and designs. These limit access to the membrane insert and the ability to perform 3D invasion assay in customized devices. Recently, 3D cell culture has gained traction in the development of invasion assays due to its ability to mimic the *in vivo* metastatic conditions [4]. Various researchers have developed spheroid-based invasion assays. However, those methods are time-consuming, costly, and labor-intensive due to the step of spheroid formation before the treatment of chemoattractants and the end-point evaluation of invasive cells [5,6]. Therefore, alternative materials are required to increase the flexibility to perform 3D invasion assays.

Because of its microfibrous structure, paper can support cells in a 3D environment [7–9]. Furthermore, paper is biocompatible and easy to

* Corresponding author.
** Corresponding author at: Biosensors and Bioanalytical Technology for Cells and Innovative Testing Device Research Unit, Department of Clinical Chemistry, Faculty of Allied Health Sciences, Chulalongkorn University, Bangkok, Thailand.
E-mail addresses: jemn@dtu.dk (J. Emnéus), Wanida.L@chula.ac.th (W. Laiwattanapaisal).

https://doi.org/10.1016/j.sbsr.2020.100354
Received 30 March 2020; Received in revised form 19 May 2020; Accepted 20 May 2020

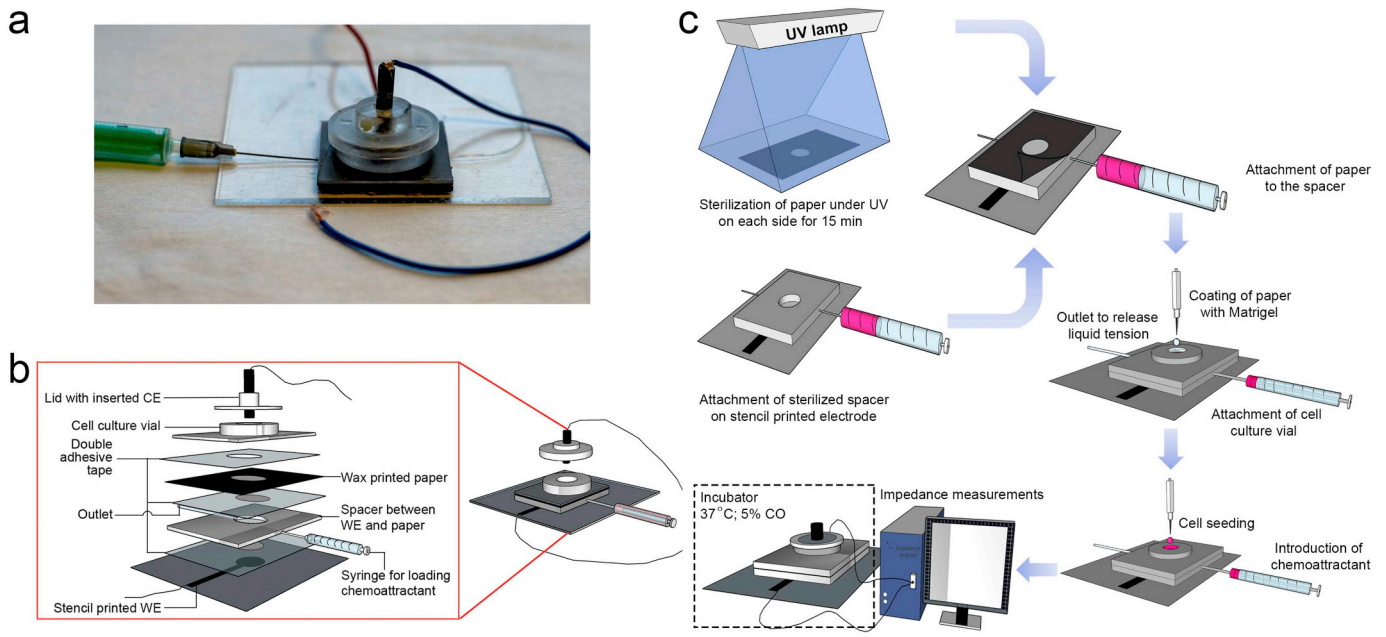

Fig. 1. a) An image of the fabricated invasion assay device, b) Schematic diagram representing the layers of the fabricated invasion assay device (left) and the assembled device (right), and c) Experimental setup of the real-time invasion assay device for B16 melanoma 4A5 cells under IGF-1 treatment.

use for device assembly. For these reasons, paper has been employed as a cell culture substrate in various applications, such as drug discovery [10], disease modeling [8,9,11–15], and cell cryopreservation [16,17]. The cell culture zone can be easily patterned using wax printing and sterilized by UV before cell seeding. Mosadegh et al. demonstrated a paper-based invasion assay by constructing a device containing multiple layers of paper. Fluorescently labeled cells were then encapsulated in a gel and placed in the middle of the stacked multilayer [18]. However, this approach requires a paper destacking step to analyze the invading cells in each layer. Paper-based 3D cell culture devices have also been coupled with electrochemical measurements. Lei et al. demonstrated paper-based 3D cell culture for quantifying cell proliferation using Electrochemical Impedance Spectroscopy (EIS) [19,20], which shows the potential of paper as an alternative scaffold for 3D cell cultures in combination with electrochemical techniques.

EIS has been widely used for label-free real-time cellular studies [21]. When cells are seeded on an electrode surface, adherent cells act as insulators, which impedes the passage of alternating current. An increasing number of cells on an electrode surface results in a corresponding increasing impedance. This principle has been used to develop different real-time migration and invasion assay devices. For example, the commercial xCELLigence system was used for invasion study. For instance, the invasion of melanoma and colorectal cancer cells under the treatment of conditioned medium from adipocytes. The cell culture wells were separated into two compartments by a porous membrane. Before performing the invasion assay, the membrane was coated with Matrigel followed by addition of the conditioned medium in the lower compartment. The dynamics of cancer invasion was then studied over time using impedance measurements without the need for cell labeling [22]. Other than the commercial devices, researchers have miniaturized the invasion assay using a microfluidic setup. The microfluidic system provides a convenient invasion platform as well as a reliable quantitative measurement of invasive cells [23–25]. For instance, Toh et al. have developed a polydimethylsiloxane (PDMS)-made microfluidic device. The device consists of three perfusion channels, which allow medium, cells, and chemoattractant loading. Perfusion of the medium, the microenvironment within the device, and the 3D cell formation could mimic the invasive mechanism close to the *in vivo* environment [26]. EIS was used in a simple invasion assay by integrating the electrodes in a transwell-inspired device [27]. The assay was performed by placing chemoattractant under the membrane insert and cellular invasion was followed in real time by an increasing impedance due to the movement of cells.

To provide a more accessible real-time invasion assay based on the 3D formation of cells, we developed an invasion assay device using easy fabrication processes. Owing to the developed wax printing [28] and stencil-printing technique [29], we could fabricate paper-based cell culture and working electrode (WE) conveniently using general laboratory instruments. CNC micromilling was applied for the fabrication of culture chambers and lid. To monitor the invasion of cells through the pores of the paper, counter electrode (CE) and WE were placed above and below the paper, respectively, without any contacts. Paper was coated with Matrigel before seeding cells on top and introducing the chemoattractant below. The device functioned as a sterile closed system using the CE built-in lid. The device was then applied for the invasion study of B16 melanoma 4A5 cells under the treatment of insulin growth factor-1 (IGF-1). Cell invasion was monitored based on the blockage of the current flow caused by invasive cells in the paper pores. This resulted in an increased impedance magnitude. Melanoma invasion was confirmed using scanning electron microscopy (SEM) and confocal 3D *Z*-stack imaging and compared with a conventional transwell assay. As a result of the paper-based scaffold, the invasion of cells could be studied based on the 3D formation of cells.

2. Materials and methods

2.1. Cells and reagents

B16 melanoma 4A5 cells from mouse, Dulbecco's Modified Eagle's medium (DMEM), fetal bovine serum (FBS), 100× penicillin/streptomycin, 0.25% trypsin-EDTA solution, Insulin growth factor-1 (IGF-1), potassium hexacyanoferrate(II/III), and Phosphate Buffered Saline (PBS) were purchased from Sigma-Aldrich Corporation (Merck KGaA, St. Louis, MO, USA). Calcein-AM was purchased from Invitrogen. Propidium iodide (PI) was purchased from BioLegend. Matrigel was purchased from Corning (Corning Incorporated, NY, USA). Sodium hydroxide (NaOH) was purchased from Merck Millipore (Darmstadt, Germany).

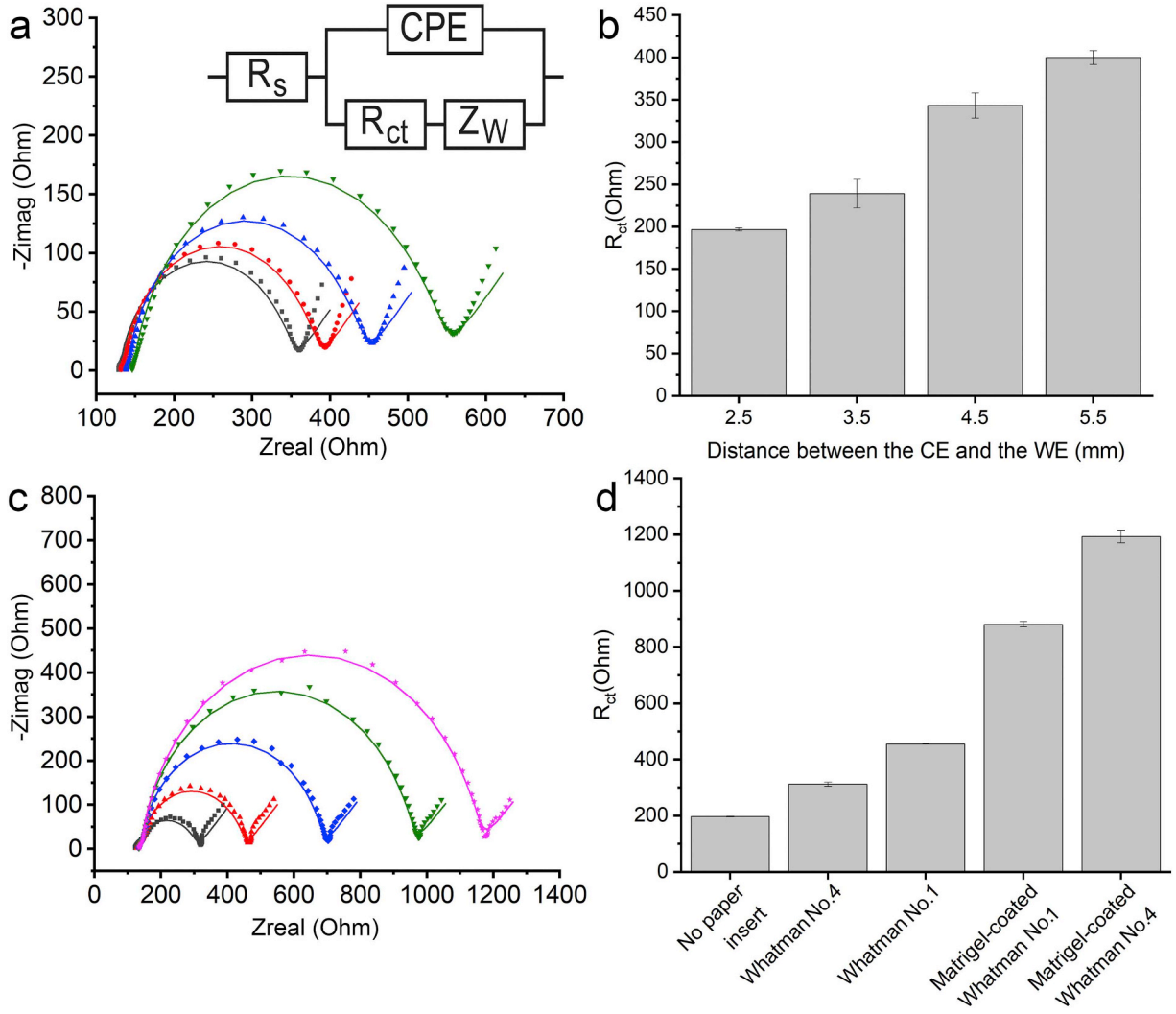

Fig. 2. a) Nyquist plots acquired at different distances between the CE and the WE: 2.5 (■ black), 3.5 (● red), 4.5 (▲ blue), and 5.5 (▼ green) mm and b) their average R_{ct} when characterized in different device assemblies, c) Nyquist plots acquired for the invasion assay device without paper (■ black) insert as well as with paper insert: Whatman No. 4 (▲ red), Whatman No. 1 (◆ blue), Matrigel-coated Whatman No. 1 (▼ green), and Matrigel-coated Whatman No. 4 (★ magenta), and d) their average R_{ct} when characterized in different device assemblies. The solid lines represent curve fitting to the equivalent circuit in the inset. Data in the bar graph are presented as the mean ± SD (n = 3). (For interpretation of the references to colour in this figure legend, the reader is referred to the web version of this article.)

2.2. Paper preparation for use as a membrane insert

Patterning of Whatman cellulose filter paper No. 1 and No. 4 (Sigma-Aldrich) was designed using Photoshop CS4 software. The paper insert was 40 × 40 mm^2 and consisted of one 10 mm wide circular cell culture zone in the center (Fig. 1). A Xerox ColorQube 8870 printer was used to print wax patterns on one side of the filter papers. The wax-patterned paper inserts were baked on a hot plate at 150 °C for 2 min to allow the wax to melt and penetrate through the thickness of the paper. After cooling, the wax solidified in the paper forming a hydrophobic barrier [28].

2.3. Device fabrication

The invasion assay device consisted of four layers (a schematic view of the details is shown in Fig. 1b): (1) a stencil-printed carbon WE on poly(methyl methacrylate) (PMMA) substrate, (2) a PMMA spacer between the electrodes, (3) a wax-printed paper insert as a culture substrate for melanoma cells, and (4) a PMMA cell culture vial. The PMMA sheet for electrode printing had dimensions of 100 × 100 mm^2 and thickness of 1.5 mm. The other layers had dimensions of 40 × 40 mm^2. The cell culture vial was covered with a plastic lid made of PMMA, specially designed to enable the insertion of a glassy carbon (GC) rod (Ø 5 mm) from Alfa Aesar (Lancashire, UK) to be used as a CE. A wire as an electrical connection to the CE was attached using Epotek H20E conductive silver-filled epoxy glue (Epoxy Technology, Inc., Billerica, MA, USA) followed by baking at ca 70 °C for at least 2 h.

The cell culture vial, spacer between the WE and paper insert, and plastic lid were designed using Autodesk Inventor Professional 2019. The designs were then converted to G-code using CimatronE 12.0 software and fabricated using a CNC micromilling machine. The cell culture vial had a total volume of 628 µl and was designed as an 8 mm high cylinder with an inner diameter of 10 mm (the outer diameter was 30 mm). The PMMA spacer between the WE and the paper insert had a central hole of 10 mm in diameter and thickness of 1.5 mm to form a chemoattractant-containing lower chamber, into which melanoma cells could invade through the paper. The spacer also had two 1 mm wide micromilled channels (one channel on each side of the spacer) leading to the central hole. The channel on the upper side was interfaced to 800 µm Teflon tubing (inner diameter 300 µm) to release the liquid tension within the spacer chamber. The channel on the lower side was interfaced with a sterile hypodermic syringe needle for medium or

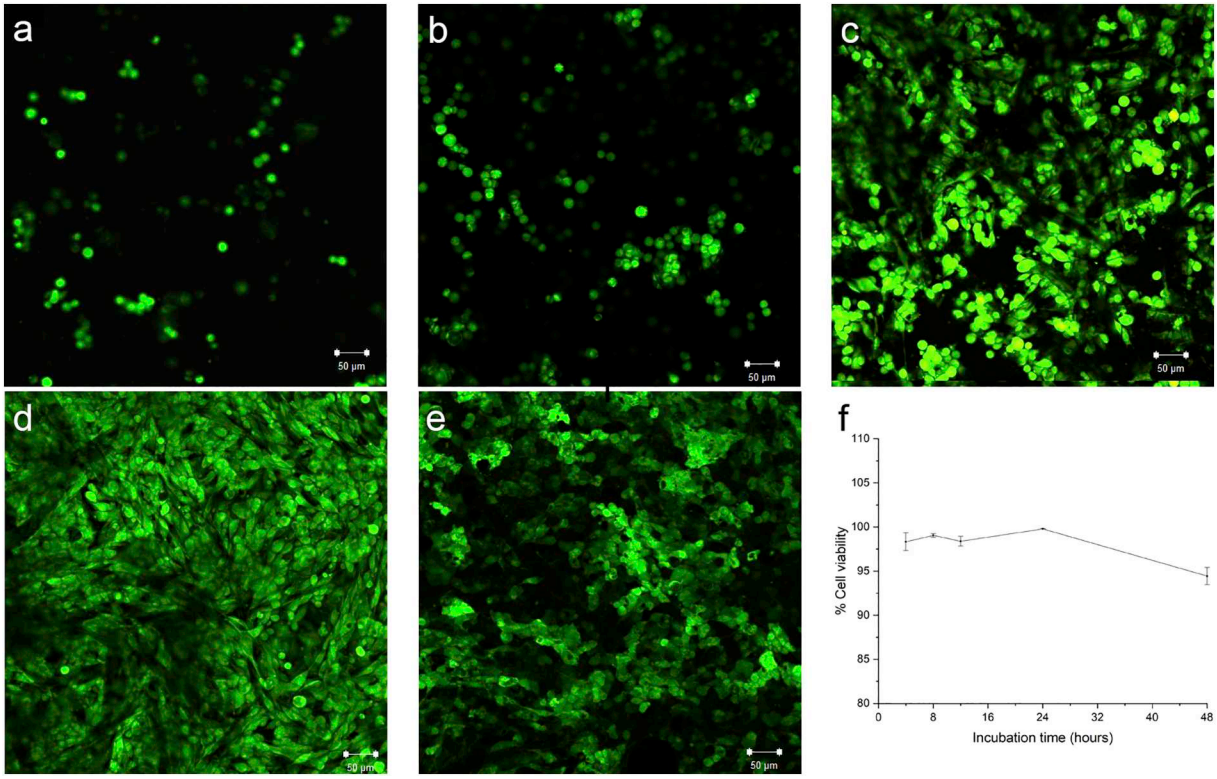

Fig. 3. Viability assessment of B16 melanoma 4A5 cells on a paper insert in the assembled device: Confocal microscopy images of LIVE/DEAD stained cells after a) 4, b) 8, c) 12, d) 24, and e) 48 h (green – calcein-AM; red – propidium iodide; scale bars: 50 µm). f) % Cell viability. Data are presented as the mean ± SD (n = 3). (For interpretation of the references to colour in this figure legend, the reader is referred to the web version of this article.)

chemoattractant loading. Both the syringe needle (Ø 0.8 mm) and the Teflon tubing were attached to the spacer channels using Sylgard 184 PDMS at 1:10 ratio of the curing agent:silicone elastomer base.

SWT 20 + R semiconductor wafer processing tape (75 µm thickness) from Nitto Belgium NV was used to create a stencil for printing the carbon WE on the PMMA substrate. The printed carbon structure (designed using CorelDRAW X8) comprised a circular WE (Ø 10 mm) and a 43 × 4 mm^2 rectangular part that served as a lead and contact pad. After attaching the tape to the PMMA substrate, the shape of the structure to be printed was cut using an Epilog Mini 18 CO_2 laser cutter with 100% speed, 15% power, and frequency of 2500 Hz (Epilog Laser, Golden, CO, USA). The used laser parameters allowed cutting of the tape without affecting the PMMA substrate. Subsequently, the laser-cut tape was peeled off in the area where the carbon electrode structure was to be formed followed by spreading of the carbon sensor paste without the use of mesh screen (Code no. C2030519P4, SunChemical). The carbon sensor paste was spread using a PDMS squeegee. The stencil was peeled off either immediately after spreading of the carbon paste or after a 24 h precuring period. The carbon paste was cured at room temperature (RT) for 72 h before assembling the device. Optimization of the stencil-printing process can be found in the supplementary information (Fig. S-1). For the electrical connection of the WE, a wire was attached to the contact pad of the electrode using Epotek H20E. The components of the device were assembled using double-sided silicone adhesive tape (INT TA106 from Intertronics, Oxfordshire, UK) that was laser cut (15% power, 100% speed, and frequency of 2500 Hz) according to the dimensions of the device. A schematic view of the assembly is shown in Fig. 1.

2.4. EIS characterization of the device

EIS measurements were used to characterize the different steps in device construction: Optimization of the (1) stencil printing of carbon WEs, (2) distance between the WE and GC CE, (3) choice of paper for the insert (Whatman filter papers No. 1 and No. 4 from GE Healthcare), and (4) effect of Matrigel coating (from a 500 µg/ml solution in sterile 0.7% NaCl for 2 h at 37 °C) of the paper insert. The measurements were performed in PBS containing 10 mM potassium hexacyanoferrate(II/III) using a PalmSens4 potentiostat (PalmSens BV, Houten, The Netherlands). Impedance spectra were acquired by applying a 10 mV_{rms} sinusoidal potential over a frequency range of 100 Hz to 1 MHz (10 points per decade). Initially, for characterizing the performance of the stencil-printed WEs, a gold-coated silicon plate (10 × 25 mm^2) was used as the CE. During characterization of the paper inserts (before and after Matrigel coating) in an assembled device, 450 µl and 150 µl of the potassium hexacyanoferrate(II/III) solution was introduced in the upper and lower compartments, respectively.

2.5. Cell culturing

B16 melanoma 4A5 cells were cultured in standard T75 cm^2 flasks using DMEM supplemented with 10% FBS, 2 mM L-glutamine, 100 U/ml penicillin/streptomycin. Cell cultures were maintained at 37 °C in a humidified incubator with 5% CO_2. Before seeding cells on the paper, cell suspensions were prepared by standard trypsinization using a 0.25% trypsin-EDTA solution. Cells were centrifuged at 200g (25 °C) for 5 min. The cell number was determined using a NucleoCounter NC-200. The desired cell densities were prepared by diluting the initial cell suspension with the culture medium.

2.6. Device preparation and invasion assay

After fabrication of the device components, the stencil-printed WE, spacer, and cell culture vial were sterilized by soaking in 500 mM NaOH for 15 min followed by rinsing twice in PBS and water. The sterilized components were air-dried before assembly. The wax-printed paper was

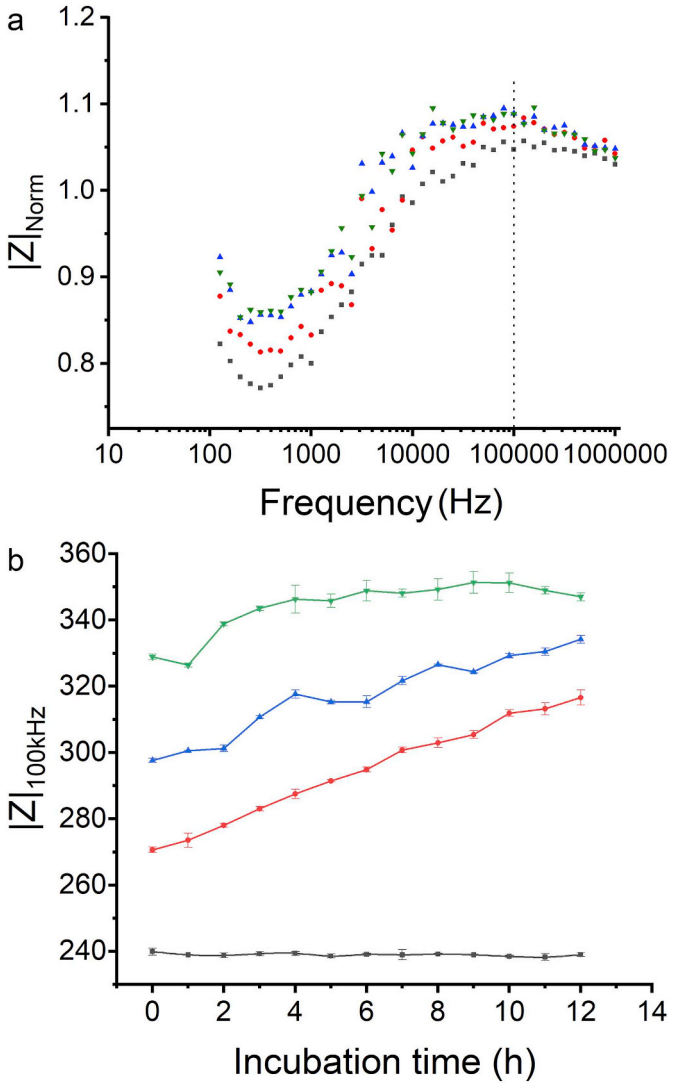

Fig. 4. Impedance characteristics of the invasion assay device in the presence of B16 melanoma 4A5 cells: a) the relationship between normalized impedance magnitude ($|Z|_{Norm}$) and log frequency after 3 (■ black), 6 (● red), 9 (▲blue), and 12 (▼green) hours of incubation, showing the maximum at 100 kHz for each time point, and b) the impedance magnitude at 100 kHz ($|Z|_{100kHz}$) over time after seeding 25,000 (■ black), 50,000 (● red), 500,000 (▲blue), and 1,000,000 (▼green) cells/cm^2. Data are presented as the mean ± SD (n = 3). (For interpretation of the references to colour in this figure legend, the reader is referred to the web version of this article.)

sterilized under UV for 15 min on each side. All the preparation steps and the device assembly (see Section 2.3) were done on a laminar flow bench. Before cell seeding, the paper insert was coated with Matrigel (see Section 2.4). 450 µl of cell suspension in DMEM without FBS was placed in the cell culture vial (upper compartment). 150 µl of DMEM without FBS was injected into the lower compartment. The device was closed with the lid having the inserted GC CE. Cells were stabilized by incubating at 37 °C in a humidified incubator with 5% CO_2 atmosphere for 24 h. After that, the medium in the lower compartment was replaced by 150 µl of culture medium containing either IGF-1 (100 ng/ml) without FBS or only FBS. The device was kept at 37 °C in a humidified incubator with 5% CO_2 atmosphere throughout the experiment. EIS measurements (PalmSens4 potentiostat) were performed using the same parameters as described in Section 2.4. Cellular invasion through the paper was tracked by acquiring an impedance spectrum every 1 h for 47 h in total (Fig. 1c).

2.7. Impedance data analysis

To monitor the invasion of cells through the thickness of paper over time, the change in the impedance magnitude was converted into cell index (CI) using Eq. (1) [30],

$$\text{Cell index (CI)} = \max_{i=1,2,\ldots,N} \frac{|Z(t,f_i)| - |Z(0,f_i)|}{|Z(0,f_i)|}, \quad (1)$$

where $|Z(t,f_i)|$ is the impedance magnitude at a specific frequency and time point and $|Z(0,f_i)|$ is the impedance magnitude at the same frequency at the time immediately after cell seeding. To determine the frequency at which the maximum value of CI was obtained, impedance spectra were acquired at different time points and the relationship between normalized impedance magnitude (Eq. 2) and log frequency was studied.

$$\text{Normalized impedance magnitude} = \frac{|Z(t,f_i)|}{|Z(0,f_i)|} \quad (2)$$

2.8. Cell viability assay on the paper insert

After the device was assembled, 800,000 B16 melanoma 4A5 cells in 450 µl culture medium were seeded on Matrigel-coated paper insert in the upper compartment and cultured as described above. The medium was changed every 24 h. After 4, 8, 12, 24, and 48 h of incubation, a solution containing calcein-AM and PI (both at 4 µg/ml in PBS) was added to the upper compartment and kept for 20 min at 37 °C in the incubator. The paper with the stained cells was then removed from the device with a scalpel and washed with PBS twice before imaging with a Zeiss LSM 700 confocal microscope. Fluorescent images were captured in five fields and the intensity of calcein-AM and PI in each image was analyzed using ImageJ software. The average intensity of calcein-AM and PI of the five captured images was calculated and converted to the percentage of cell viability using the ratio of live cells to the total number of cells.

3. Results and discussion

3.1. Choice of the counter electrode and its placement in the device

In two-electrode applications of EIS, the area of a CE is conventionally larger than that of the WE to ensure that the primary contribution to the measured impedance is due to the WE [31]. Moreover, in conventional applications, the placement of the WE and CE would also have a higher degree of freedom. For the application and device we present here, the main criterion for choosing a CE was to ensure that the impedance measurements through a membrane would effectively map changes in the entire membrane area caused by cell migration. Hence, the CE area should be rather similar to that of the stencil-printed WE and the center of the CE should be aligned with that of the WE [32]. Although the gold-coated silicon plate (10 × 25 mm^2) CE was sufficient for the preliminary electrode characterization, it could not meet the above-mentioned requirements. A GC rod (Ø 5 mm) was considered sufficient and could be easily placed concentrically with the stencil-printed WE, meeting the above-mentioned requirements.

The PMMA lid of the device was designed to facilitate placement of the GC rod in the center of the device and easy attachment using nylon screws inserted from the left and right side of the GC rod (Fig. S-2), which also allowed fast adjustment of the distance between the CE and WE. To evaluate the influence of the distance on impedance measurements, the GC rod was adjusted at distances of 2.5, 3.5, 4.5, and 5.5 mm from the WE. Fig. 2a and b shows Nyquist plots that indicate how R_{ct} increased with distance. 2.5 mm was the shortest feasible distance to have sufficient space for the paper insert. Because the PMMA spacer is 1.5 mm thick, this distance ensures that the tip of the CE was approximately 1 mm from the surface of the paper insert. Therefore, we

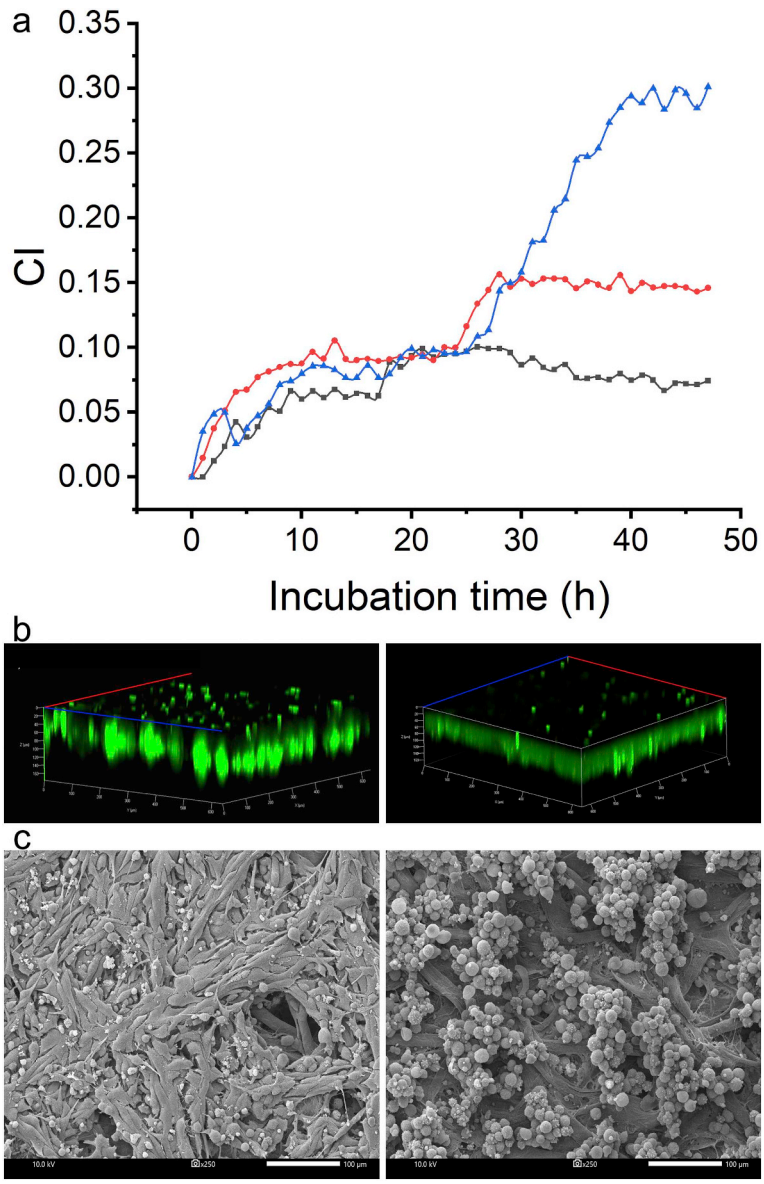

Fig. 5. a) CI *vs* incubation time for B16 melanoma 4A5 cells (initial cell seeding density of 1,000,000 cells/cm^2), showing a stable baseline when the cells were maintained in culture medium without FBS for the first 24 h, and an increase in CI (from 25 to 47 h) when the medium in the lower compartment was replaced by DMEM with only FBS (● red) or 100 ng/ml IGF-1 (▲blue) (no increase in CI for the negative control (■ black)). b, c) Microscope images showing B16 melanoma 4A5 cell behavior on a paper insert in the absence (left) and presence (right) of IGF-1: b) Confocal microscopy 3D *Z*-stack images (green – calcein-AM; red – propidium iodide); c) SEM images (scale bar 100 μm). (For interpretation of the references to colour in this figure legend, the reader is referred to the web version of this article.)

chose to fix the GC rod at a distance of 2.5 mm from the WE.

3.2. Choice of paper for the membrane insert

To choose the optimal paper for the membrane insert, Whatman filter paper was considered due to its a) cellulose component, which easily allows wax printing; b) ability to support 3D cell culture [7]; c) the purity of the paper (Whatman No. 1 and No. 4 contain ≤0.06% ash); and d) stability during long-term soaking in culture medium for up to 120 h [7]. We tested Whatman No. 1 and Whatman No. 4 filter papers due to their pore sizes (11 μm and 20–25 μm, respectively), which would match the size of melanoma cells (~10 μm), making cell penetration possible.

After device assembly, impedance measurements were performed with and without a paper insert. The results showed that upon the insertion of paper, the average R_{ct} was higher than without paper insert due to the obstruction of the current flow by the paper. Moreover, when using Whatman No. 4 as the insert, the average R_{ct} was lower than was obtained for Whatman No. 1 insert. This can be attributed to the larger pore size of Whatman No. 4, which impeded the current flow less than Whatman No. 1. Subsequently, we evaluated the influence of Matrigel coating on the two paper inserts. The results showed that the presence of Matrigel acted as an additional insulator, increasing the R_{ct} in comparison with the values obtained for naked paper inserts. Furthermore, we observed that the average R_{ct} for Matrigel-coated Whatman No. 4 was higher than that for Whatman No. 1 (Fig. 2c and d). This behavior may be explained based on the larger porosity of Whatman No. 4 paper, which allowed the diluted Matrigel to penetrate readily through the entire thickness of the paper. Hence, Whatman No. 1 was chosen to be used as the membrane insert in our device due to the lower R_{ct} after Matrigel coating.

3.3. Cell viability and morphology assessment of the paper insert

To confirm the biocompatibility of our device, 800,000 B16 melanoma 4A5 cells in 450 μl of culture medium were seeded and cultured on Matrigel-coated Whatman No. 1 paper insert. LIVE/DEAD staining was then performed after 4, 8, 12, 24, and 48 h of incubation.

Confocal images were obtained to confirm the viability of the cells cultured in the device (Fig. 3a–e). This result confirms the biocompatibility of our device for the total period needed for performing invasion assays. After 4, 8, and 12 h of incubation, the cells were still in circular shape and did not fully attach and spread onto the paper. Therefore, the cells were washed out when we removed the medium for LIVE/DEAD

staining, resulting in the low cell density as shown in Fig. 3a. After 24 h of incubation, the cells had fully attached to the paper and acquired a fibroblast-like shape (Fig. 3d). On the other hand, after 48 h of incubation, the cells had passed through the entire thickness of the paper due to the presence of FBS in the culture medium, which could activate cell invasion (Fig. 3e and S-3). Fig. 3f shows a summary of the viability assessment, indicating that even after 48 h incubation more than 90% of the cells remained viable. This result suggested that after seeding, the cells required a 24 h stabilization period in FBS containing culture medium before the chemoattractant treatment and impedance measurements could be started.

3.4. Impedance characteristics of the device in the presence of cells

For the cell-based impedance system, the biggest change of the impedance signal is observed at various frequencies, depending on the sensitivity of the sensor [33]. To determine the frequency at which the highest impedance is obtained in our system, 800,000 B16 melanoma 4A5 cells in 450 μl of culture medium were seeded on the paper insert in the assembled device. After that, we performed the impedance measurements every hour for 12 h. Fig. 4a shows the normalized impedance magnitude (Eq. 2) as a function of log frequency based on the impedance spectra acquired after 3, 6, 9, and 12 h incubation. The result indicated that the highest impedance magnitude was obtained at approximately 100 kHz, which was then chosen for the subsequent experiments.

EIS-based cellular assays require the optimization of cell seeding density to obtain an impedance baseline that allows easy evaluation of how the cells respond to the introduced drug or other effectors [34]. To determine the cell density that provides an optimal baseline impedance before introduction of the chemoattractant, we suspended 20,000, 40,000, 400,000, and 800,000 B16 melanoma 4A5 cells in 450 μl of culture medium and seeded them on the Matrigel-coated paper insert in the device. The chosen cell seeding densities correspond to 25,000, 50,000, 500,000, and 1,000,000 cells/cm^2. Subsequently, impedance spectra were acquired every hour for 12 h. Fig. 4b shows the impedance magnitude at 100 kHz as a function of incubation time for each cell seeding density. The initial impedance magnitude immediately after cell seeding (0 h) clearly increased with increasing cell seeding density. During the 12 h incubation period, the cell density of 25,000 cells/cm^2 did not increase impedance, indicating that the cell density would be below the limit of detection. The two intermediate cell densities, 50,000 and 500,000 cells/cm^2, led to monotonically increasing impedance, which would not provide a proper baseline for an assay. On the other hand, in the case of 1,000,000 cells/cm^2, the determined impedance was highest and reached a plateau which provided a clear initial baseline before introduction of the chemoattractant. The high impedance magnitude at 0 h of 1,000,000 cells/cm^2 was caused by a very high concentration in medium suspension, resulting in the high resistance in the system right after seeding. However, the value dropped after the system was stable after 1 h of incubation. Moreover, the higher initial impedance would also improve the sensitivity of impedance monitoring during cell invasion. Based on the above assessment, 1,000,000 cells/cm^2 was chosen as the cell density for the invasion assay.

3.5. 3.5 Invasion assay of B16 melanoma 4A5 cells

IGF-1 has been implicated in metastasis of melanoma through increased production of Interleukin-8 [35]. Melanoma patients have also been identified with an upregulated IGF-1 receptor content [36]. Because of the significance of IGF-1 to melanoma invasion, the developed device was used for the invasion study under IGF-1 treatment at a concentration of 100 ng/ml based on a previous report [37]. The result was compared with cell migration in the presence of only FBS and without FBS (negative control).

According to the initial cell morphology observed during the LIVE/DEAD staining, cells needed to be stabilized by incubating them for 24 h in culture medium without FBS before applying the chemoattractant. Fig. 5a shows that after the first 24 h of incubation, the cells showed a relatively similar CI baseline. During that period, the CI slightly increased due to cell adhesion on the paper insert. After 24 h, the lower compartment was filled with medium containing 10% FBS or 100 ng/ml IGF-1 while the impedance measurements were continued. In the case of the negative control, the lower compartment was filled with medium without any added FBS or IGF-1. The obtained results indicated that after 25 h incubation in medium without FBS the CI did not show any increase; in fact, it slightly decreased during the last 20 h of incubation. In the presence of FBS, the CI showed a slight increase but leveled off after only a few hours. On the other hand, when IGF-1 was introduced, a threefold increase in CI could be observed. The observed increased CI after the treatment of FBS and IGF-7 in this experiment was caused by the penetration of cells into the pore of the paper, which resulted in an additional impediment of current flow within the system. Thus, the more extensive the observed cell invasion is, the more obstruction to the current is caused by the cells penetrating within the pores of the paper, concomitantly increasing the measured impedance. This phenomenon is analogous to what was observed when the pores of paper inserts were filled with Matrigel coating, which resulted in an increased impedance (Fig. 2c and d). Moreover, the EIS measurements could distinguish the effect of the treatment (IGF-1 or FBS) on B16 melanoma 4A5 cell invasion already after 7 h. According to the hallmarks of cancer, cell motility and their ability to invade extracellular matrix (ECM) are the key aspects of cell invasion [38]. The invasion of B16 melanoma 4A5 cells on the paper insert was confirmed by *Z*-stack imaging using confocal microscopy (Fig. 5b) and SEM (Fig. 5c). After 12 h treatment with medium containing 10% FBS or 100 ng/ml IGF-1, the cells were stained with calcein-AM and PI. Based on confocal microscopy imaging, there were fewer cells on the surface of the paper after IGF-1 treatment. The fluorescence intensity of the stained cells through the entire thickness of the paper was higher in the case of IGF-1 treatment (Fig. 5b, right panel) in comparison with the cells that were only exposed to medium without FBS (Fig. 5b, left panel), which confirmed that the invasion was enhanced by IGF-1. Fig. 5c (left) shows multiple layers of cells with a flattened shape on the paper when only medium without FBS was introduced, indicating the inability of cells to invade through the ECM on the paper. On the other hand, Fig. 5c (right) shows cells with round shape, which were able to invade ECM and penetrate through the pores of the paper as a response to IGF-1 treatment, indicating the formation of spheroids of cells during cell invasion. Furthermore, the EIS results correlated well with the conventional transwell assay (Fig. S-3). However, real-time EIS measurements allowed monitoring of the kinetics of cell invasion instead of only an end-point measurement. The conventional invasion assay requires at least 12 h of incubation after the introduction of chemoattractants, whereas the real-time EIS-based invasion assay could reduce the incubation time to 7 h, also making it more reliable because the shorter incubation time decreases the influence of cell proliferation [2]. In this experiment, we demonstrated the applicability of the device to the detection of melanoma invasion under IGF-1 treatment. These results lead us to the development of a multiwell device in the future, to perform high-throughput experiments.

4. Conclusions

To make real-time invasion assay devices more accessible, in this work, we have demonstrated an alternative material, paper, as a membrane insert for invasion assay. The use of paper could reduce the cost of real-time invasion assay experiments. Importantly, the paper provides the 3D culture environment for the melanoma cells and allows spheroid formation. Besides, the use of paper allows easy customization to fit different cell culture devices. To eliminate the need for cell

labeling and counting steps to investigate invasive cells, we coupled the use of Matrigel-coated paper (membrane insert) with real-time EIS measurements. Using real-time EIS measurements, the IGF-1-induced invasion of B16 melanoma 4A5 cells on the paper could be distinguished from a negative control faster than using a conventional transwell assay. Hence, the invasion study was less affected by cell proliferation. The pore size of the filter paper was a crucial factor in determining the suitable paper for the EIS-based invasion assay. Filter paper with an intermediate pore size (~11 μm) comparable to the size of melanoma cells resulted in lower background impedance upon Matrigel coating, allowing more sensitive detection of the impedance changes caused by cell invasion into the pores of the paper. Though the paper is not transparent, the confirmation of cell invasion, cell viability assay, and visualization could be performed directly on the paper using fluorescent staining. The paper could be easily cut out using a scalpel before imaging. Here, we first demonstrate the effect of cell invasion through ECM and pores of paper, which can be detected by the impedance signal. In this regard, we provide another perspective of invasion assay through the use of paper-based cell culture with impedance monitoring. Our device can also be developed for high-throughput measurements by increasing the number of culture wells. A paper membrane could be designed to have a pattern of multiple cell culture zones.

Declaration of Competing Interest

The authors declare that they have no known competing financial interests or personal relationships that could have appeared to influence the work reported in this paper.

Acknowledgments

N. P. gratefully acknowledges the Thailand Research Fund and National Research Council of Thailand through the Royal Golden Jubilee Ph.D. Program (under grant no. PHD/0012/2558). This research was financially supported by the Thailand Research Fund through Research Team Promotion Grant (RTA6080002).

Appendix A. Supplementary data

Supplementary data to this article can be found online at https://doi.org/10.1016/j.sbsr.2020.100354.

References

[1] D. Rosel, M. Fernandes, P. Veselý, P. Heneberg, V. Čermák, A. Gandalovičová, et al., Migrastatics—anti-metastatic and anti-invasion drugs: promises and challenges, Trends Cancer 3 (2017) 391–406, https://doi.org/10.1016/j.trecan.2017.04.008.
[2] J. Marshall, Transwell® invasion assays, Cell Migration, Springer, 2011, pp. 97–110, https://doi.org/10.1007/978-1-61779-207-6_8.
[3] A. Teresiak, M. Kapałczyńska, T. Kolenda, W. Przybyła, M. Zajączkowska, V. Filas, et al., 2D and 3D cell cultures–a comparison of different types of cancer cell cultures, Arch Med Sci 14 (2018) 910, https://doi.org/10.5114/aoms.2016.63743.
[4] E. Sahai, Mechanisms of cancer cell invasion, Curr Opin Genet Dev 15 (2005) 87–96, https://doi.org/10.1016/j.gde.2004.12.002.
[5] M. Vinci, C. Box, S.A. Eccles, Three-dimensional (3D) tumor spheroid invasion assay, JoVE (2015) e52686, https://doi.org/10.3791/52686.
[6] J.M. Holy, A.T. Riegel, A. Wellstein, E.B. Berens, A cancer cell spheroid assay to assess invasion in a 3D setting, JoVE 10 (2015) e53409, https://doi.org/10.3791/53409.
[7] N. Pupinyo, M. Chatatikun, A. Chiabchalard, W. Laiwattanapaisal, *In situ* paper-based 3D cell culture for rapid screening of the anti-melanogenic activity, Ananlyst 144 (2019) 290–298, https://doi.org/10.1039/c8an01725e.
[8] R. Derda, A. Laromaine, A. Mammoto, S.K. Tang, T. Mammoto, D.E. Ingber, et al., Paper supported 3D cell culture for tissue-based bioassays, PNAS 106 (2009) 18457–18462, https://doi.org/10.1073/pnas.0910666106.
[9] R. Derda, S.K. Tang, A. Laromaine, B. Mosadegh, E. Hong, M. Mwangi, et al., Tissue Papers: leveraging paper-based microfluidics for the next generation of 3D tissue models, Plos One 6 (2011) e18940, https://doi.org/10.1371/journal.pone.0018940.
[10] F. Liu, S. Ge, J. Yu, M. Yan, X. Song, Electrochemical device based on a Pt nanosphere-paper working electrode for *in situ* and real-time determination of the flux of H_2O_2 releasing from SK-BR-3 cancer cells, Chem. Commun. 50 (2014) 10315–10318, https://doi.org/10.1039/C4CC04199B.
[11] S.M. Cramer, T.S. Larson, M.R. Lockett, et al., Tissue Papers: leveraging paper-based microfluidics for the next generation of 3D tissue models, Anal. Chem. (2019) 10916–10926, https://doi.org/10.1021/acs.analchem.9b02102.
[12] R.M. Kenney, M.W. Boyce, A.S. Truong, C.R. Bagnell, M.R. Lockett, Real-time imaging of cancer cell chemotaxis in paper-based scaffolds, Analyst 141 (2016) 661–668, https://doi.org/10.1039/c5an01787d.
[13] B.E. Dabiri, M.R. Lockett, B. Mosadegh, R. Derda, P. Campbell, K.K. Parker, et al., Three-dimensional paper-based model for cardiac ischemia, Adv. Healthc Mater. 3 (2014) 1036–1043, https://doi.org/10.1002/adhm.201300575.
[14] M.C. Sapp, H.J. Fares, A.C. Estrada, K.J. Grande-Allen, Multilayer three-dimensional filter paper constructs for the culture and analysis of aortic valvular interstitial cells, Acta Biomater. 13 (2015) 199–206, https://doi.org/10.1016/j.actbio.2014.11.039.
[15] Y. Wei, Q. Zhang, C. Bin, G.T. Liang, L. Wei-Xuan, Z. Xiao-Mian, et al., Study on microenvironment acidification by microfluidic chip with multilayer-paper supported breast cancer tissue, Chinese J. Anal. Chem. 41 (2013) 822–827, https://doi.org/10.1016/S1872-2040(13)60661-1.
[16] Y. Kim, S. Uhm, M. Gupta, J. Yang, J.G. Lim, Z. Das, et al., Successful vitrification of bovine blastocysts on paper containe, Theriogenology 78 (2012) 1085–1093, https://doi.org/10.1016/j.theriogenology.2012.05.004.
[17] K.H. Lee, J.C. Sun, C.K. Chuang, S.F. Guo, C.F. Tu, J.C. Ju, An efficient and mass reproducible method for vitrifying mouse embryos on a paper in cryotubes, Cryobiology 66 (2013) 311–317, https://doi.org/10.1016/j.cryobiol.2013.03.009.
[18] M.R. Lockett, K.T. Minn, B. Mosadegh, K.A. Simon, K. Gilbert, S. Hillier, et al., A paper-based invasion assay: assessing chemotaxis of cancer cells in gradients of oxygen, Biomaterials 53 (2015) 262–271, https://doi.org/10.1016/j.biomaterials.2015.02.012.
[19] K.F. Lei, C.H. Huang, N.M. Tsang, Impedimetric quantification of cells encapsulated in hydrogel cultured in a paper-based microchamber, Talanta 147 (2016) 628–633, https://doi.org/10.1016/j.talanta.2015.10.052.
[20] K.F. Lei, T.K. Liu, N.M. Tsang, Towards a high throughput impedimetric screening of chemosensitivity of cancer cells suspended in hydrogel and cultured in a paper substrate, Biosens. Bioelectron. 100 (2018) 355–360, https://doi.org/10.1016/j.bios.2017.09.029.
[21] S. Tonello, E. Cantù, M. Marziano, G. Abate, M. Vezzoli, W. Rungratanawanich, et al., Monitoring Caco-2 to enterocyte-like cells differentiation by means of electric impedance analysis on printed sensors, Biochim. Biophys. Acta 1863 (2019) 893–902, https://doi.org/10.1016/j.bbagen.2019.02.008.
[22] J.Y. Um, S.G. Lee, W.M. Yang, J.H. Ko, G. Sethi, K.S. Ahn, Conditioned media from adipocytes promote proliferation, migration, and invasion in melanoma and colorectal cancer cells, J. Cell. Physiol. 234 (2019) 18249–18261, https://doi.org/10.1002/jcp.28456.
[23] K.F. Lei, H.P. Tseng, C.Y. Lee, N.M. Tsang, Quantitative study of cell invasion process under extracellular stimulation of cytokine in a microfluidic device, Sci. Rep. 6 (2016) 1–8, https://doi.org/10.1038/srep25557.
[24] C.M. Oefner, Y. Abbas, W.J. Polacheck, L. Gardner, L. Farrell, A. Sharkey, et al., A microfluidics assay to study invasion of human placental trophoblast cells, J. R. Soc. Interface 14 (2017) 20170131, https://doi.org/10.1098/rsif.2017.0131.
[25] Z. Guo, T. Yu, H. Fan, J. Song, Y. Liu, Z. Gao, et al., Cancer-associated fibroblasts promote non-small cell lung cancer cell invasion by upregulation of glucose-regulated protein 78 (GRP78) expression in an integrated bionic microfluidic device, Oncotarget 7 (2016) 25593–25666, https://doi.org/10.18632/oncotarget.8232.
[26] Y.C. Toh, A. Raja, H. Yu, D. Van Noort, A 3D microfluidic model to recapitulate cancer cell migration and invasion, Bioengineering 5 (2018) 29, https://doi.org/10.3390/bioengineering5020029.
[27] M.S. Chiriacò, F. Dioguardi, E. Primiceri, A.G. Monteduro, E. D'Amone, R. Rinaldi, et al., Automatic transwell assay by an EIS cell chip to monitor cell migration, Lab Chip 11 (2011) 4081–4086, https://doi.org/10.1039/c1lc20540d.
[28] E. Carrilho, A.W. Martinez, G.M. Whitesides, Understanding wax printing: a simple micropatterning process for paper-based microfluidics, Anal. Chem. 81 (2009) 7091–7095, https://doi.org/10.1021/ac901071p.
[29] M.A. Pellitero, M. Kitsara, F. Eibensteiner, F.J. del Campo, Rapid prototyping of electrochemical lateral flow devices: stencilled electrodes, Analyst 141.8 (2016) 2515–2522, https://doi.org/10.1039/C5AN02424B.
[30] X. Wang, X. Xu, K. Solly, B. Strulovici, W. Zheng, Application of real-time cell electronic sensing (RT-CES) technology to cell-based assays, Assay Drug Dev. Technol. 2 (2004) 363–372, https://doi.org/10.1089/adt.2004.2.363.
[31] J.H. Sluyters, On the impedance of galvanic cells: I. theory, Recueil Des Travaux Chimiques Des Pays-Bas 79 (1960) 1092–1100, https://doi.org/10.1002/recl.19600791013.
[32] A.R. Kolli, M.B. Esch, H.E. Abaci, B. Srinivasan, M.L. Shuler, J.J. Hickman, TEER measurement techniques for *in vitro* barrier model systems, J. Lab Autom. 20 (2015) 107–126, https://doi.org/10.1177/2211068214561025.
[33] A. Yúfera, A. Olmo, P. Daza, D. Cañete, Cell biometrics based on bio-impedance measurements, Adv. Biometric Technol. 17 (2011) 343–366, https://doi.org/10.

5772/21742.
[34] C. Caviglia, K. Zor, S. Canepa, M. Carminati, L.B. Larsen, R. Raiteri, et al., Interdependence of initial cell density, drug concentration and exposure time revealed by real-time impedance spectroscopic cytotoxicity assay, Analyst 140 (2015) 3623–3629, https://doi.org/10.1039/c5an00097a.
[35] G. Li, B. Vaidya, J. Kalabis, M. Herlyn, K. Satyamoorthy, Insulin-like growth factor-I-induced migration of melanoma cells is mediated by interleukin-8 induction, Cell Growth Differ. 13 (2002) 87–93.
[36] C. All-Ericsson, L. Girnita, S. Seregard, A. Bartolazzi, M.J. Jager, O. Larsson, Insulin-like growth factor-1 receptor in uveal melanoma: a predictor for metastatic disease and a potential therapeutic target, IOVS 43 (2002) 1–8.
[37] A. Girnita, C. All-Ericsson, M.A. Economou, M. Axelson, S. Seregard, O. Larsson, et al., The insulin-like growth factor-I receptor inhibitor picropodophyllin causes tumor regression and attenuates mechanisms involved in invasion of uveal melanoma cells, Clin. Cancer Res 12 (2006) 1383–1391, https://doi.org/10.1111/j.1755-3768.2008.01183.x.
[38] D. Hanahan, R.A. Weinberg, Hallmarks of cancer: the next generation, Cell 144 (2011) 646–674, https://doi.org/10.1016/j.cell.2011.02.013.